B_8B_8 INTERACTION IN THE SU_6 QUARK MODEL AND ITS APPLICATIONS TO FEW-BODY SYSTEMS*

Y. FUJIWARA,[1] K. MIYAGAWA [2] M. KOHNO[3] Y. SUZUKI[4] AND C. NAKAMOTO,[5]

[1]*Department of Physics, Kyoto University, Kyoto 606-8502, Japan*
E-mail: fujiwara@ruby.scphys.kyoto-u.ac.jp
[2]*Department of Applied Physics, Okayama Science University, Okayama 700-0005, Japan*
[3]*Physics Division, Kyushu Dental College, Kitakyushu 803-8580, Japan*
[4]*Department of Physics, Niigata University, Niigata 950-2181, Japan*
[5]*Suzuka National College of Technology, Suzuka 510-0294, Japan*

The recent QCD-inspired spin-flavor SU_6 quark model for the baryon-baryon interaction, proposed by the Kyoto-Niigata group, is a unified model for the complete baryon octet ($B_8 = N$, Λ, Σ and Ξ), which has achieved very accurate description of the NN and YN interactions. These quark-model interactions are now applied to realistic calculations of few-body systems in a new three-cluster Faddeev formalism which uses the 2-cluster resonating-group method kernel explicitly. We review the essential features of the most recent models, fss2 and FSS, and their predictions to few-body systems in confrontation with the available experimental data. As the few-body systems, we discuss the three-nucleon bound states, $2\alpha\Lambda$ system for ${}^{9}_{\Lambda}$Be, and $2\Lambda\alpha$ system for ${}^{6}_{\Lambda\Lambda}$He.

1. Introduction

An important purpose of studying baryon-baryon interactions in the quark model (QM) is to obtain the most accurate understanding of the fundamental strong interaction in a natural picture, in which the short-range part of the interaction is relevantly described by the quark-gluon degree of freedom and the medium- and long-range parts by dominated meson-exchange processes. In the spin-flavor SU_6 QM, the baryon-baryon interactions for all the octet baryons ($B_8 = N,\ \Lambda,\ \Sigma$ and Ξ) are treated entirely equivalently with the well-known nucleon-nucleon (NN) interaction. We have recently

*This work is supported by a Grant-in-Aid for Scientific Research (C) from Japan Society for the Promotion of Science (JSPS) (No. 15540270).

proposed a comprehensive QM description of general baryon-octet baryon-octet (B_8B_8) interactions, which is formulated in the $(3q)$-$(3q)$ resonating-group method (RGM) using the spin-flavor SU_6 QM wave functions, a colored version of the one-gluon exchange Fermi-Breit interaction, and effective meson-exchange potentials (EMEP's) acting between quarks.[1-5] The early version, the model FSS,[1-3] includes only the scalar (S) and pseudoscalar (PS) meson-exchange potentials as the EMEP's, while the renovated one fss2 [4,5] introduces also the vector (V) meson-exchange potentials and the momentum-dependent Bryan-Scott terms for the S and V mesons. Owing to these improvements, the model fss2 in the nucleon-nucleon (NN) sector has attained the accuracy comparable to that of one-boson exchange potentials (OBEP's).

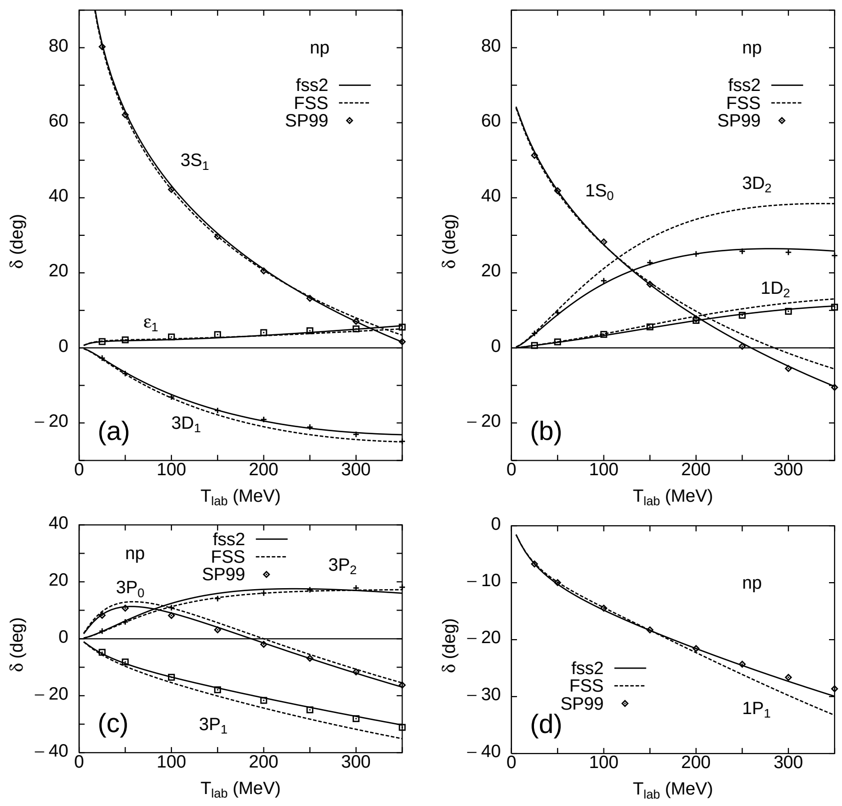

Figure 1. Comparison of np phase shifts for $J \leq 2$ with the phase-shift analysis SP99 by Arndt *et al.*[10] The solid curves are the results by fss2 and the dotted curves by FSS.

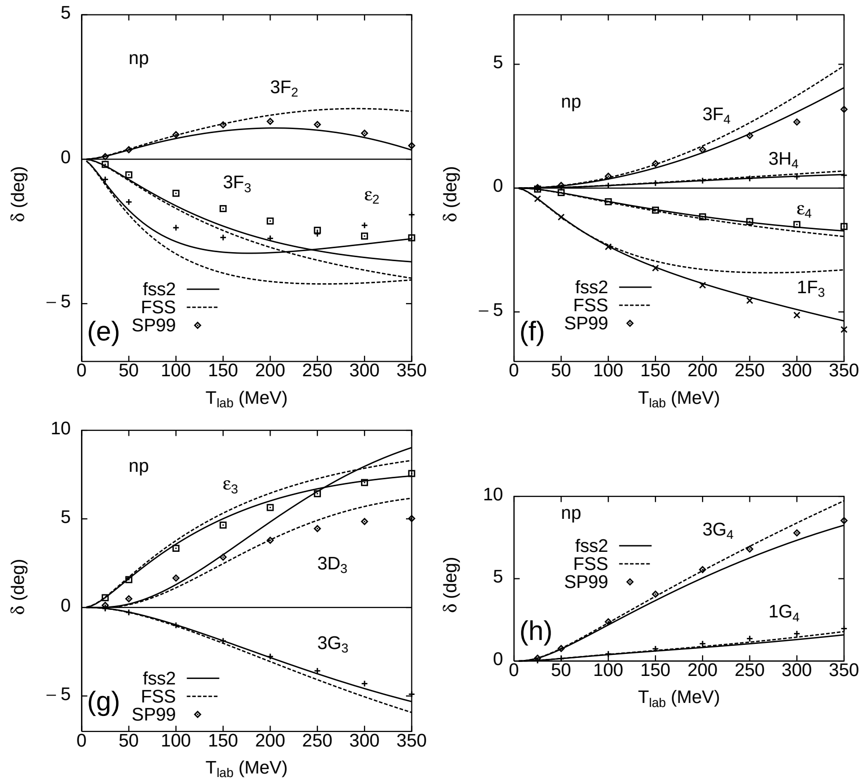

Figure 2. The same as Fig. 1 but for higher partial waves with $J \leq 4$.

These QM potentials can now be used for various types of many-body calculations, which include the G-matrix calculations [6] of baryonic matter and the Faddeev calculations of few-baryon systems.[7] For this purpose, we have recently developed a new 3-cluster formalism which uses two-cluster RGM kernel explicitly.[8] The proposed equation entirely eliminates 3-cluster redundant components by the orthogonality of the total wave function to the pairwise two-cluster Pauli-forbidden states. The explicit energy dependence inherent in the exchange RGM kernel is self-consistently determined. This equation is entirely equivalent to the Faddeev equation which uses a modified singularity-free T-matrix (which we call the RGM T-matrix) constructed from the two-cluster RGM kernel. We first applied this formalism to a 3-dineutron system and the 3α system, and obtained a complete agreement between the Faddeev calculation and the variational calculation which

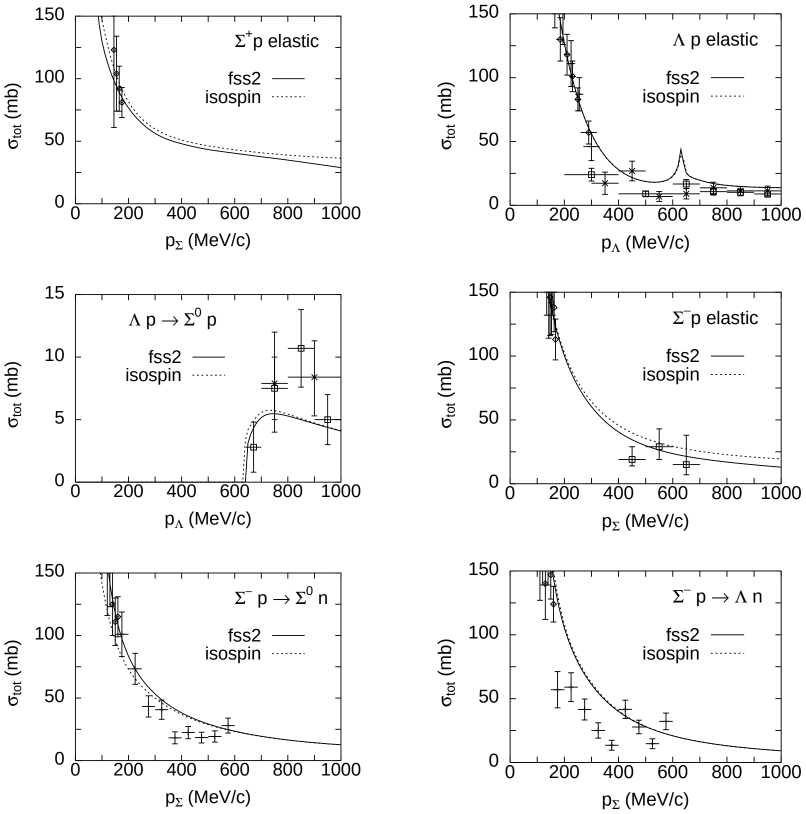

Figure 3. Calculated YN total cross sections compared with the available experimental data.

uses the translationally invariant harmonic-oscillator (h.o.) basis.[8,9] Here we apply the formalism to the Faddeev calculations of the 3-nucleon ($3N$) bound state,[7] as well as $2\alpha\Lambda$ and $2\Lambda\alpha$ systems.

2. B_8B_8 interactions by fss2

Figures 1 and 2 display some important low-partial wave NN phase-shift parameters predicted by the model fss2, in comparison with the phase shift analysis SP99.[10] The previous results by FSS are also shown with the dotted curves. Due to the inclusion of V mesons, the NN phase shifts of the fss2 at the non-relativistic energies up to $T_{\rm lab} = 350$ MeV are greatly improved, and now have attained the accuracy almost comparable to that of one-boson exchange potentials. The good reproduction of the NN phase-shift parameters in fss2 continues up to $T_{\rm lab} \sim 600$ MeV,[4] where the inelasticity of the S-matrix becomes appreciable.

The total cross sections of the YN scattering predicted by fss2 are compared with the available experimental data in Fig. 3. The "total" cross sections for the scattering of charged particles (i.e., pp, Σ^+p and Σ^-p systems) are calculated by integrating the differential cross sections over $\cos\theta_{\rm min} = 0.5 \sim \cos\theta_{\rm max} = -0.5$. The solid curves indicate the result in the particle basis, while the dashed curves in the isospin basis. In the latter case, the effects of the charge symmetry breaking, such as the Coulomb effect and the small difference of the threshold energies for Σ^-p and Σ^0n channels, are neglected. New experimental data for Σ^-p elastic total cross sections at the intermediate energies, p_Σ = 400-700 MeV/c, measured at KEK,[11] are consistent with the fss2 predictions.

The Σ^+p differential cross sections at the intermediate energy $p_\Sigma =$ 450 MeV/c are compared with the KEK experiment [12] in the left panel of Fig. 4. We need more experimental data to increase the statistics, in order to see which model is the most appropriate. In the right panel, the polarization observables for the Σ^+p elastic scattering at $p_\Sigma = 800$ MeV/c are shown for the models fss2 and FSS. The recent experimental data from KEK-PS 457 [13] imply the asymmetry parameter $a^{\rm exp} = 0.44 \pm 0.2$ at $p_\Sigma = 800 \pm 200$ MeV/c, which is not inconsistent with our quark-model predictions although the specific scattering angle is not possible to be identified.

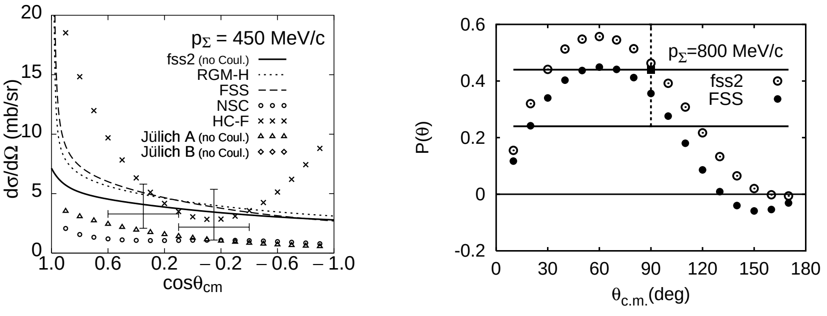

Figure 4. Left: Σ^+p differential cross sections at $p_\Sigma = 450$ MeV/c predicted by various models. The experimental data are from Ref. [12]. Right: Σ^+p poralization at $p_\Sigma =$ 800 MeV/c, predicted by fss2 and FSS. For the experiment, see the text.

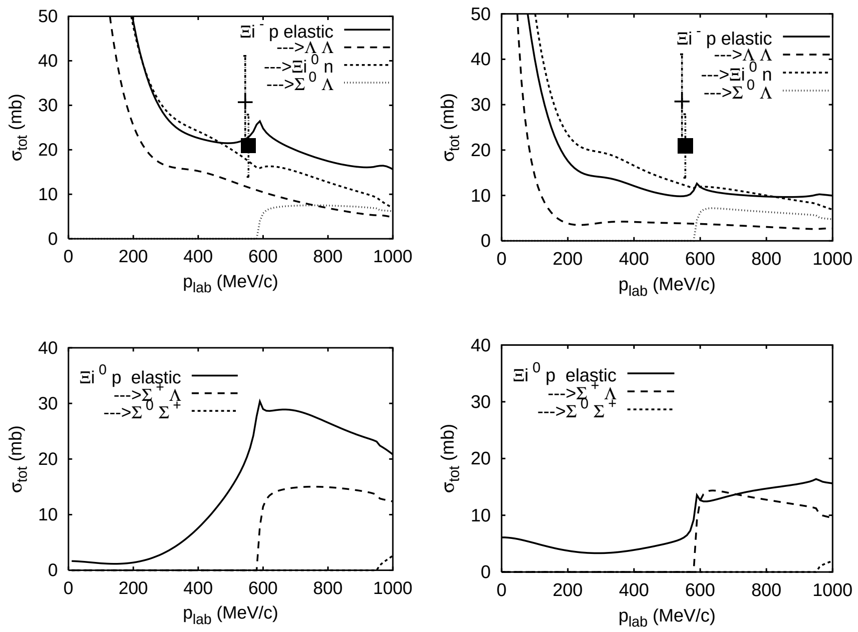

Figure 5. $\Xi^- p$ and $\Xi^0 p$ total cross sections predicted by FSS (left) ans fss2 (right). For $\Xi^- p$ cross sections both of the isospin $I = 0$ and 1 channels contribute, while for $\Xi^- n$ (or $\Xi^0 p$) only $I = 1$ channel contributes. The Coulomb force is neglected.

We show some comparison of the $\Xi^- N$ total cross sections which are recently obtained from the BNL-E906 experiment.[14] The in-medium $\Xi^- N$ total cross sections around the momentum region $p_{\rm lab} \sim 550$ MeV$/c$ are estimated as $\sigma_{\Xi N}(\text{in medium}) = 30{\pm}6.7^{+3.7}_{-3.6}$ mb. More detailed analysis using the Eikonal approximation [15] gives $\sigma_{\Xi N}(\text{in medium}) = 20.9 \pm 4.5^{+2.5}_{-2.4}$ mb. They have also estimated the cross section ratio $\sigma_{\Xi^- p}/\sigma_{\Xi^- n} = 1.1^{+1.4+0.7}_{-0.7-0.4}$. If we compare these experimental data with the FSS and fss2 predictions depicted in Fig. 5, we find that the FSS predictions in the left panels seem to be more favorable. However, we definately need more experimental data with higher statistics.

We summarize the characteristics of the $B_8 B_8$ interactions predicted by the model fss2 as follows.

- There is no bound state in the $B_8 B_8$ system, except for the deuteron.
- $\Xi\Xi$ total cross sections are not so large as the NN total cross sections.
- ΞN interaction has a strong isospin dependence like the ΣN interaction.
- $\Xi^- \Sigma^-$ (namely, $\Xi\Sigma(I = 3/2)$) interaction is fairly attractive.

Some of these features are very much different from the Nijmegen predictions given by Stoks and Rijken.[16]

3. Faddeev calculation for the three-nucleon bound state

The 3-cluster Faddeev formalism using the 2-cluster RGM kernel was applied to the 3-nucleon bound state, where the off-shell T-matrices derived from the non-local and energy-dependent RGM kernel for our quark-model NN interactions, fss2 and FSS, are employed.[7] The model fss2 yields the ground-state energy $E(^3\mathrm{H}) = -8.519$ MeV in the 50 channel calculation,[17] which seems to be overbound in comparison with the experimental value $E^{\mathrm{exp}}(^3\mathrm{H}) = -8.48$ MeV. In fact, this is not the case, since the present calculation uses the np interaction for each nucleon pair, which is more attractive than the nn interaction. The effect of the charge dependence is estimated to be 0.19 MeV.[18] If we take this into account, our result is still 150 keV less bound. The charge rms radii for ^{3}H and ^{3}He are also correctly reproduced. These results are the closest to the experiments among many results obtained by Faddeev calculations, employing modern realistic NN interactions. A non-local description of the short range correlations in the quark model is essential to reproduce the large binding energy and the correct size of the three-nucleon bound state without reducing the D-state probability of the deuteron.

4. $2\alpha\Lambda$ Faddeev calculation for $^9_\Lambda$Be

As a typical example of three-cluster systems composed of two identical clusters, we apply the present formalism to the $2\alpha\Lambda$ Faddeev calculation

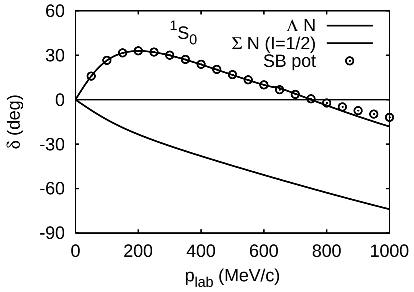

Figure 6. ΛN $^1S_0$ phase shifts by fss2 (solid curve) and by SB potential (Circles).

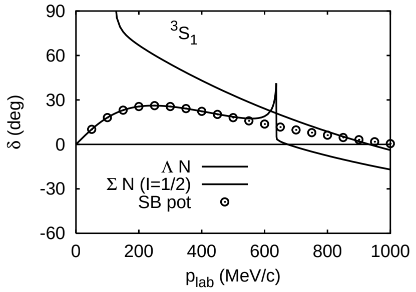

Figure 7. The same as Fig. 6, but for the $^3S_1$ phase shifts.

for ${}^{9}_{\Lambda}$Be, using the 2α RGM kernel and the $\Lambda\alpha$ folding potential constructed from a simple ΛN effective interaction. For the 2α RGM kernel, we use the the 3-range Minnesota force [19] with the exchange mixture $u = 0.946869$, and the h.o. width parameter, $\nu = 0.257$ fm^{-2}, assumed for the $(0s)^4$ α-clusters. The 2α phase shifts are nicely reproduced in the 2α RGM calculation, using this effective NN interaction. For the 3α system, we find that the 3α ground-state energy obatined by solving the present 3α Faddeev equation is only about 1.5 MeV higher than that of the full microscopic 3α RGM calculation.[9] The effective ΛN interaction, denoted by SB (Sparenberg-Baye potential) in Table 1, is constructed from the ${}^1S_0$ and ${}^3S_1$ phase shifts predicted by the YN sector of the model fss2, by using an inversion method based on supersymmetric quantum mechanics.[20] These are simple 2-range Gaussian potentials which reproduce the low-energy behaviour of the ΛN phase shifts in Figs. 6 and 7, obtained in the full coupled-channel calculations:

$$V_{{}^1S_0}(r) = -128.0\ \exp(-0.8908\ r^2) + 1015\ \exp(-5.383\ r^2)\ \ ,$$
$$V_{{}^3S_1}(r) = -56.31\, f\ \exp(-0.7517\ r^2) + 1072\ \exp(-13.74\ r^2)\ \ ,$$

where $V(r)$ in MeV and r in fm. In the ${}^3S_1$ state, the phase-shift behavior only in the low-momentum region with $p_{\rm lab} < 600$ MeV/c is fitted, since the cusp structure is never reproduced in the single-channel calculation. Since any central and single-channel effective ΛN force leads to the well-

Table 1. The ground-state energy $E_{\rm gr}(0^+)$ and the 2^+ excitation energy $E_{\rm x}(2^+)$ in MeV, calculated by solving the Faddeev equation for the $2\alpha\Lambda$ system. For the effective NN force for the 2α RGM kernel, the 3-range Minnesota force is used. The ΛN force, SB, stands for the Sparenberg-Baye potential and NS - JB are the G-matrix based effective forces used by Hiyama *et al.*[23] The experimental values are from Ref. [24].

$V_{\Lambda N}$	$E_{\rm gr}(0^+)$ (MeV)			$E_{\rm x}(2^+)$
	ours	Hiyama	diff.	(MeV)
SB	-6.837	–	–	2.915
NS	-6.742	-6.81	0.07	2.916
ND	-7.483	-7.57	0.09	2.935
NF	-6.906	-7.00	0.09	2.930
JA	-6.677	-6.76	0.08	2.919
JB	-6.474	-6.55	0.08	2.911
Exp't	-6.62 ± 0.04			3.029(3)/3.060(3)

known overbinding problem of ${}^{5}_{\Lambda}$He by about 2 MeV (in the present case, it is 1.63 MeV), the attractive part of the ${}^3S_1$ ΛN potential is modified to reproduce the correct binding energy, $E^{\rm exp}({}^{5}_{\Lambda}{\rm He}) = -3.12 \pm 0.02$ MeV, with an adjustable parameter $f = 0.8923$. This overbinding problem is mainly attributed to the Brueckner rearrangement effect of the α-cluster, originating from the starting energy dependence of the bare two-nucleon interaction due to the addition of an extra Λ particle.[22] The odd-state ΛN interaction is assumed to be zero. The partial waves up to $\lambda_{\rm Max} = \ell_{1\,{\rm Max}} = 6$ are included both in the 2α and $\Lambda\alpha$ channels. The direct and exchange Coulomb kernel between two α-clusters is introduced at the nucleon level with the cut-off radius, $R_C = 14$ fm. Table 1 shows the ground-state (0^+) and the 2^+ excitation energies of ${}^{9}_{\Lambda}$Be, predicted by the SB and the other various ΛN potentials used by Hiyama *et al.*[23]. In the present calculations using only the central force, the SB potential with the pure Serber character can reproduce the the ground-state and the excitation energies within the accuracy of 100 - 200 keV.

5. $2\Lambda\alpha$ Faddeev calculation for ${}^{6}_{\Lambda\Lambda}$He

Next, we use the $\Lambda\alpha$ T-matrix, used in the $2\alpha\Lambda$ Faddeev calculation, to calculate the ground-state energy of ${}^{6}_{\Lambda\Lambda}$He. The full coupled-channel T-matrices of fss2 and FSS with the strangeness $S = -2$ and the isospin $I = 0$ are employed for the $\Lambda\Lambda$ RGM T-matrix. Table 2 shows the $\Delta B_{\Lambda\Lambda}$ values (in MeV) defined by $\Delta B_{\Lambda\Lambda} = B_{\Lambda\Lambda}({}^{6}_{\Lambda\Lambda}{\rm He}) - 2B_{\Lambda}({}^{5}_{\Lambda}{\rm He})$. $V_{\Lambda\Lambda}$(Hiyama) uses the 3-range Gaussian potential in Ref. [23].

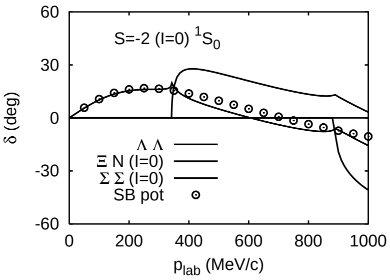

Figure 8. $\Lambda\Lambda$ ${}^1S_0$ phase shifts by fss2 (solid curve) and by SB potential (Circles).

We find that the Hiyama's 3-range Gaussian $\Lambda\Lambda$ potential [23] and our Faddeev calculation using FSS yield very similar results with the large $\Delta B_{\Lambda\Lambda}$ values about 3.6 MeV, since the $\Lambda\Lambda$ phases shifts predicted by these interactions increase upto about 40°. The improved quark model fss2 yields $\Delta B_{\Lambda\Lambda} = 1.41$ MeV. (If we use the $\Lambda\Lambda$ single-channel T-matrix, this number is reduced to $\Delta B_{\Lambda\Lambda} = 1.14$ MeV.) In Table 2, the result denoted by $V_{\Lambda\Lambda}$(SB) is by the 2-range Gaussian potential generated from the fss2 ${}^1S_0$ $\Lambda\Lambda$ phase shift (Fig. 8) in the full-channel calculation, using the supersymmetric inversion method.[20] This potential is explicitly given by

$$V_{\Lambda\Lambda}(\mathrm{SB}) = -103.9\ \exp(-1.176\ r^2) + 658.2\ \exp(-5.936\ r^2)\ \ ,$$

where $V_{\Lambda\Lambda}(\mathrm{SB})$ in MeV and r in fm. We think that the 0.5 MeV difference between our fss2 result and the $V_{\Lambda\Lambda}(\mathrm{SB})$ result is probably because we neglected the full coupled-channel effect of the $\Lambda\Lambda\alpha$ channel to the $\Xi N\alpha$ and $\Sigma\Sigma\alpha$ channels. We should also keep in mind that in all of these 3-cluster calculations the Brueckner rearrangement effect of the α-cluster with the magnitude of about -1 MeV (repulsive) is very important.[25] It is also reported in Ref. [26] that the quark Pauli effect between the α cluster and the Λ hyperon plays as a non-negligible repulsive contribution of the order of 0.1 - 0.2 MeV for the Λ separation energy of ${}^{\ 6}_{\Lambda\Lambda}\mathrm{He}$, even when we assume a rather compact $(3q)$ size of $b = 0.6$ fm. Taking all of these effects into consideration, we can conclude that the present results by fss2 are in good agreement with the recent experimental value, $\Delta B^{\mathrm{exp}}_{\Lambda\Lambda} = 1.01 \pm 0.20$ MeV,[27] deduced from the Nagara event.

6. Summary

We have extended the $(3q)$-$(3q)$ RGM study of the the NN and YN interactions [1-4] to the strangeness $S = -2,\ -3$ and -4 sectors without introducing any extra parameters, and have clarified some characteristic features of the B_8B_8 interactions.[5] The results seem to be reasonable, if we consider i) the spin-flavor SU_6 symmetry, ii) the weak pion effect in the strangeness sector,

Table 2. Comparison of $\Delta B_{\Lambda\Lambda}$ values in MeV, predicted by various $\Lambda\Lambda$ interactions and $V_{\Lambda N}$ potentials. $V_{\Lambda\Lambda}$ (Hiyama) is the 3-range Gaussian potential used by Hiyama *et al.*[23] The difference between our calculation and Hiyama's calculation is also shown. FSS and fss2 use the $\Lambda\Lambda$ RGM T-matrix in the free space. $\varepsilon_{2\Lambda}$ is the 2Λ expectation value determined self-consistently. $V_{\Lambda\Lambda}(\mathrm{SB})$ is the two-range Gaussian potential given in the text. In $V_{\Lambda\Lambda}(\mathrm{SB})$ only the S-wave is used, while in the others converged results with enough partial waves are given.

	$V_{\Lambda\Lambda}$(Hiyama)			FSS		fss2		$V_{\Lambda\Lambda}$(SB)
$V_{\Lambda N}$	ours	Hiyama	diff	E	$\varepsilon_{2\Lambda}$	E	$\varepsilon_{2\Lambda}$	(S-wave)
SB	3.618	–	–	3.650	5.131	1.411	5.942	1.902
NS	3.548	3.59	0.04	3.623	5.159	1.364	5.951	1.917
ND	3.181	3.10	−0.08	3.231	4.482	1.288	5.231	1.636
NF	3.208	3.22	0.01	3.301	4.626	1.270	5.410	1.719
JA	3.370	3.44	0.07	3.468	4.908	1.306	5.705	1.833
JB	3.486	3.56	0.07	3.592	5.150	1.325	5.956	1.924

and iii) the effect of the flavor symmetry breaking. These B_8B_8 interactions are now used for the detailed study of the few-body systems, as well as baryonic matter problems, in various ways. Here we reported applications of the NN, YN and YY interactions to the Faddeev calculations of the three-nucleon bound state, the $2\alpha\Lambda$ system for ${}^{9}_{\Lambda}$Be, and the $2\Lambda\alpha$ system for ${}^{6}_{\Lambda\Lambda}$He. We find that our most recent model fss2 gives the triton binding energy large enough to compare with the experiment, without reducing the deuteron D-state probability. The charge root-mean-square radii of ^{3}H and ^{3}He are also correctly reproduced. In the application to the $2\alpha\Lambda$ system, the 2α RGM kernel with the effective Minnesota force [19] and some appropriate ΛN force generated from the low-energy phase-shift behavior of fss2 yield the the ground-state and excitation energies of ${}^{9}_{\Lambda}$Be within the accuracy of 100 - 200 keV. The weak $\Lambda\Lambda$ force $\Delta B^{\rm exp}_{\Lambda\Lambda} = 1.01 \pm 0.20$ MeV by the Nagara event [27] for ${}^{6}_{\Lambda\Lambda}$He is reasonably reproduced by the Faddeev calculation of the $2\alpha\Lambda$ system, using the present $\Lambda\alpha$ T-matrix and the full coupled-channel $\Lambda\Lambda$-ΞN-$\Sigma\Sigma$ $\widetilde{T}$-matrix of fss2.

It is important to note that the newly developed 3-cluster Faddeev formalism using the 2-cluster RGM kernel opens a way to solve few-baryon systems interacting by the quark-model baryon-baryon interaction without spoiling the essential features of the RGM kernel; i.e., the non-locality, the energy dependence and the existence of the pairwise Pauli-forbidden state. It can also be used for the 3-cluster systems involving α-clusters, like the ${}^{9}_{\Lambda}$Be and ${}^{6}_{\Lambda\Lambda}$He systems. A nice point of this formalism is that the underlying NN and YN interactions are more directly related to the structure of the hypernuclei than the models assuming simple 2-cluster potentials. In particular, we have found that the most recent quark-model interaction, the model fss2, yields a realistic description of many systems including the 3-nucleon bound state, ${}^{9}_{\Lambda}$Be and ${}^{6}_{\Lambda\Lambda}$He.

References

1. Y. Fujiwara, C. Nakamoto and Y. Suzuki, *Phys. Rev. Lett.* **76**, 2242 (1996).
2. Y. Fujiwara, C. Nakamoto and Y. Suzuki, *Phys. Rev.* C **54**, 2180 (1996).
3. T. Fujita, Y. Fujiwara, C. Nakamoto and Y. Suzuki, *Prog. Theor. Phys.* **100**, 931 (1998).
4. Y. Fujiwara, T. Fujita, M. Kohno, C. Nakamoto and Y. Suzuki, *Phys. Rev.* C **65**, 014002 (2002).
5. Y. Fujiwara, M. Kohno, C. Nakamoto and Y. Suzuki, *Phys. Rev.* C **64**, 054001 (2001).
6. M. Kohno, Y. Fujiwara, T. Fujita, C. Nakamoto and Y. Suzuki, *Nucl. Phys.* **A674**, 229 (2000).

7. Y. Fujiwara, K. Miyagawa, M. Kohno, Y. Suzuki and H. Nemura, *Phys. Rev.* C **66**, 021001 (R) (2002).
8. Y. Fujiwara, H. Nemura, Y. Suzuki, K. Miyagawa and M. Kohno, *Prog. Theor. Phys.* **107**, 745 (2002).
9. Y. Fujiwara, Y. Suzuki, K. Miyagawa, M. Kohno and H. Nemura, *Prog. Theor. Phys.* **107**, 993 (2002).
10. Scattering Analysis Interactive Dial-up (SAID), Virginia Polytechnic Institute, Blacksburg, Virginia R. A. Arndt: Private Communication.
11. Y. Kondo *et al.* (KEK-PS E289 collaboration), *Nucl. Phys.* **A676**, 371 (2000).
12. J. K. Ahn *et al.* (KEK-PS E251 collaboration), *Nucl. Phys.* **A648**, 263 (1999).
13. T. Kadowaki *et al.* (KEK-PS E452 collaboration), *Eur. Phys. J.* **A15**, 295 (2002).
14. T. Tamagawa *et al.* (BNL-E906 collaboration), *Nucl. Phys.* **A691**, 234c (2001).
15. Y. Yamamaoto, T. Tamagawa, T. Fukuda and T. Motoba, *Prog. Theor. Phys.* **106**, 363 (2001).
16. V. G. J. Stoks and Th. A. Rijken, *Phys. Rev.* C **59**, 3009 (1999).
17. Y. Fujiwara, K. Miyagawa, Y. Suzuki, M. Kohno and H. Nemura, *Nucl. Phys.* **A721**, 983c (2003).
18. R. Machleidt, Adv. Nucl. Part. Phys. **19**, 189 (1989).
19. D. R. Thompson, M. LeMere and Y. C. Tang, *Nucl. Phys.* **A286**, 53 (1977).
20. J.-M. Sparenberg and D. Baye, *Phys. Rev.* C **55**, 2175 (1997).
21. R. H. Dalitz, R. C. Herndon and Y. C. Tang, *Nucl. Phys.* **B47**, 109 (1972).
22. H. Bando and I. Shimodaya, *Prog. Theor. Phys.* **63**, 1812 (1980).
23. E. Hiyama, M. Kamimura, T. Motoba, T. Yamada and Y. Yamamoto, *Prog. Theor. Phys.* **97**, 881 (1997).
24. H. Akikawa *et al.* (BNL-E930 collaboration), *Phys. Rev. Lett.* **88**, 082501 (2002).
25. M. Kohno, Y. Fujiwara and Y. Akaishi, Phys. Rev. C **68**, 034302 (2003).
26. Y. Suzuki and H. Nemura, *Prog. Theor. Phys.* **102**, 203 (1999).
27. H. Takahashi *et al.* (KEK-PS E373 collaboration), *Phys. Rev. Lett.* **87**, 212502 (2001).